J Mar Sci Technol (2007) 12:183–189
DOI 10.1007/s00773-006-0235-4

ORIGINAL ARTICLE

Noncontact power supply for seafloor geodetic observing robot system

Jun Han · Akira Asada · Tamaki Ura
Yukinaga Yamauchi · Yasunobu Yagita
Toshihiko Maki

Received: August 18, 2006 / Accepted: October 18, 2006

Abstract A new and effective seafloor geodetic observing robot network system, which consists of several submarine stations situated in regions susceptible to interplate earthquakes, has been proposed and is under construction in Japan. Each station, equipped with an autonomous underwater vehicle (AUV) dock, is connected to a land facility by cables providing power and communication. Near the AUV dock, three or four seafloor reference stations will be set up for geodetic observations. In this system, a noncontact power supply is required for a battery-driven AUV to conduct observations for extended durations. A small, intelligent, efficient, high-power noncontact feed system of 400 W capacity with an inverting efficiency of 77% in salt water has been developed. It has been shown to be effective in a water tank experiment in which the noncontact power supply automatically fed power to an AUV for 3 days.

Key words Noncontact power supply · Autonomous underwater vehicle · Geodetic observation · Underwater observation

J. Han (✉) · A. Asada · T. Ura · T. Maki
Institute of Industrial Science, University of Tokyo, 4-6-1 Komaba, Meguro, Tokyo 153-8505, Japan
e-mail: hanjun@iis.u-tokyo.ac.jp

J. Han
Shanghai Fisheries University, Shanghai, China

Y. Yamauchi
Hokushin Electric Appliance Co., Ltd., Oono, Japan

Y. Yagita
Honda Electronics Co., Ltd., Toyohashi, Japan

Introduction

Historically, large-scale earthquakes repeatedly occur in the subduction zone in the interplate region where several plates meet in the sea surrounding Japan. Seafloor geodetic observation plays an important role in clarifying the mechanism of earthquakes occurring under the seabed by measuring the movement of the earth's crust at the seafloor within an accuracy of centimeters order. In order to improve the accuracy of geodetic observations, a new and effective seafloor geodetic observing robot network system has been proposed to replace observation ships.[1] At present, the system is under construction in Japan and research on technology development has commenced.[2–5] A power supply without a cable connection is required for a seafloor-station-based battery-driven autonomous underwater vehicle (AUV) in order to conduct seafloor geodetic observation for extended durations. Thus far, several noncontact charging systems have been studied. Recently, Kojiya et al.[6] proposed a noncontact automatic power supply system; however, its effectiveness has not yet been experimentally verified. Kawasaki et al.[7] and Fukasawa et al.[8] have described the *Marine Bird*, a new experimental AUV, and have performed docking and sea trials of the electric power supply; however, the downsizing of the inductive connector and improvement of its efficiency are still under development.

In comparison, in this study, not only have small noncontact power transmission and receiving coils ($60 \times 55 \times 55$ mm) been designed for practical use but also an intelligent and efficient high-power supply system of 400 W capacity with an inverting efficiency of 77% in salt water has been developed; embedded single-board computers are used to monitor the battery voltage, the

charging current, and the battery temperature as well as to automatically control the charging sequences. To prove that the system is effective, we housed the system in watertight cylinders and conducted a water tank experiment in which the noncontact power supply automatically fed power to an AUV for 3 days. In this article we focus on developing the recharging system; the homing and docking technology will be discussed and developed in future work.

Description of the seafloor geodetic observing robot network system

The seafloor geodetic observing robot network system comprises several submarine stations located in regions susceptible to interplate earthquakes. As shown in Fig. 1, each station with an AUV dock is connected to land stations with cables for power transmission and communication. Near the AUV dock, three or four seafloor reference stations will be set up for geodetic observation. When the sea conditions are suitable, the AUV surfaces to conduct observations. At other times, the AUV parks itself on the docking system to recharge its batteries, upload geodetic data, and download the latest mission commands through the cable network.

Configuration of the noncontact power supply system

The block diagram of the noncontact power supply system is shown in Fig. 2. The system consists of a power transmission unit and a power receiving unit. Photographs of the prototypes are shown in Figs. 3 and 4.

The power transmission unit comprises a high-frequency power transmission oscillator, a power transmission coil, a power transmission controller, and a transducer. The power receiving unit consists of a receiving coil, a rectification circuit, an analog-to-digital (A/D)

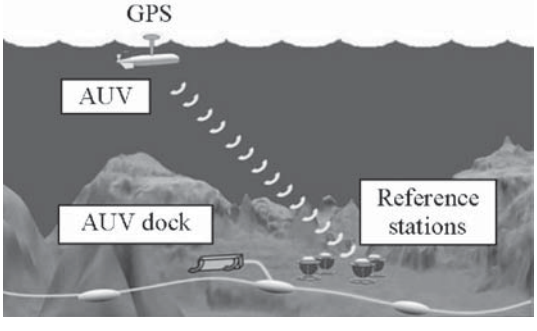

Fig. 1. Seafloor geodetic observing robot system. *GPS*, global positioning system; *AUV*, autonomous underwater vehicle

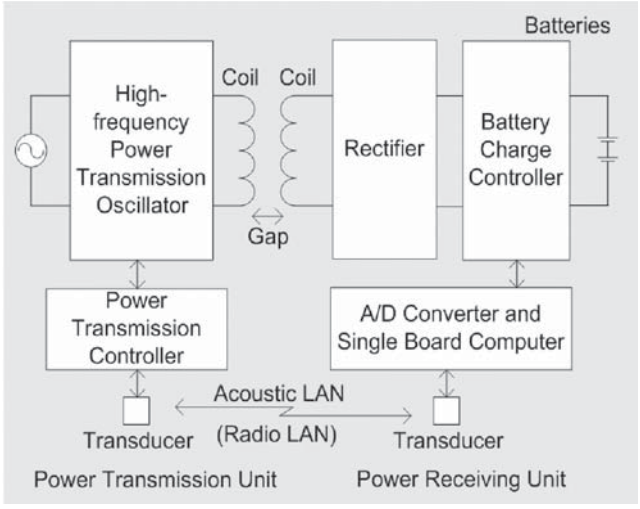

Fig. 2. Block diagram of the noncontact power supply system. *A/D*, analog to digital; *LAN*, local area network

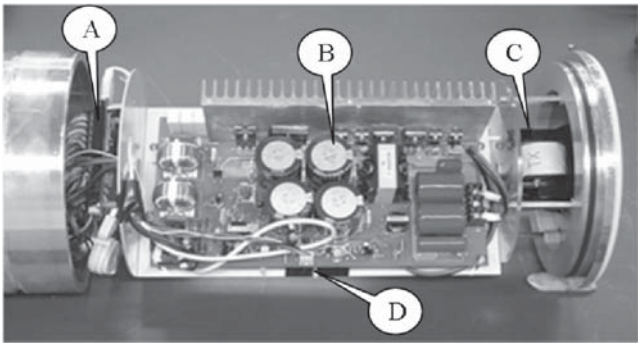

Fig. 3. Prototype power transmission unit. *A*, power transmission controller; *B*, high-frequency power transmission oscillator; *C*, power transmission coil; *D*, Universal Serial Bus (USB) radio LAN device

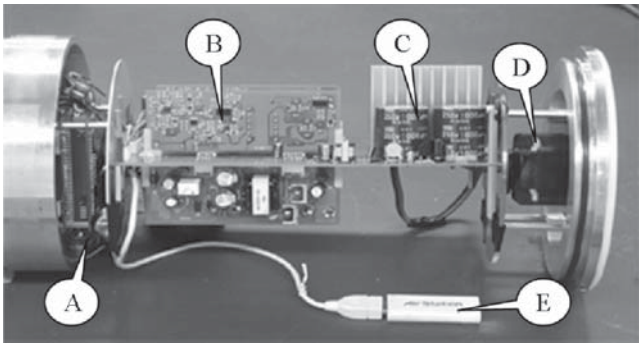

Fig. 4. Prototype power receiving unit. *A*, A/D converter and single-board computer; *B*, battery charging controller; *C*, power receiving circuit; *D*, power receiving coil; *E*, USB radio LAN device

converter, a single-board computer, a transducer, and batteries.

The power transmission coil is driven by high-frequency current at 80 kHz from the power transmission oscillator that generates a high-frequency electromagnetic field by which the receiving coil receives electric current through electromagnetic induction. The rectifier converts the high-frequency current to direct current (DC), and the batteries get charged by the charging circuit. The A/D converter and single-board computer are used for monitoring the battery voltage, the charging current, and the battery temperature as well as for controlling the charging sequences.

Small coils with dimensions of $60 \times 55 \times 55$ mm have been developed for practical use. The power transmission unit and the power receiving unit are housed in identical watertight cylinders (18 cm in diameter and 45 cm in length). Currently, the arrangement of the electronic components is not extremely compact, so it should be possible to downsize the cylinders.

Design of the power transmission and receiving unit

The selection of the operating frequency of the high-frequency generation circuit is very important. The higher the operating frequency, the smaller the size of the coil can be; however, the copper and iron losses from the electronic components increase.

High-frequency losses in the coil were almost equal to the copper losses. In order to suppress the high-frequency losses, a Litz wire twisted from a urethane-coated wire having a diameter of 0.2 mm was used. Further, the operating frequency of 80 kHz was chosen taking into consideration the heat generated and copper losses associated with the Litz wire. The number of turns of the power transmission and receiving coils were calculated and tested to obtain the best match between the coils, and they were finally set at 29 and 34 turns, respectively. By using these coils, a very high transmission efficiency (85%–88%) between the coils was successfully achieved when the gap between coils was 8–13 mm.

Battery charging control

In this system, all the charging sequences are controlled by a single-board computer embedded in the power receiving unit. Smart software has been developed for controlling battery charging in which the following features have been implemented for practical use:

— Both Ni-Cd and lithium batteries can be charged by selecting a different charging mode.

Table 1. Specifications of *Tri-Dog1*

Overall length	1.85 m
Overall breadth	0.58 m
Depth	0.53 m
Duration	>2 h
Actuators	100-W thruster × 6
Processors	Intel P MMX × 3
Batteries	25.2-V Ni-Cd 20 Ah × 4
	CH A: surge
	CH B: sway, heave, and lights
	CH C: vision CPU
	CH D: main CPU

— The charging current, voltage, and battery temperatures can be measured for charging control.
— The charging and consumption histories of the batteries can be recorded for battery management and later charging control.
— Alert functions have been formulated for dealing with any charging abnormality.
— The amount of charge supplied to the batteries is controlled to prevent overcharging and gas generation.
— There are full charge and supplementary charging modes for Ni-Cd batteries.
— Quick charging is available for lithium batteries.

Considering the charging ability (400 W) of the charger, we selected AUV *Tri-Dog1* as a suitable experimental vehicle. This vehicle is owned by the Underwater Technology Research Center, Institute of Industrial Science (IIS), University of Tokyo. As shown in Table 1, *Tri-Dog1* has four Ni-Cd battery channels for its power supply. Therefore, the noncontact power feeding system was designed to have four battery charging channels, and the Ni-Cd charging mode was used in our experiment. The Ni-Cd charging sequences are described in further detail as follows.

Two charging modes were implemented for the Ni-Cd battery, namely, full charge and supplementary charging modes. The smart software is capable of intelligently selecting the appropriate mode according to the battery status. If the battery is almost spent, full charging mode will be selected. In this mode, the battery is first discharged until it is exhausted and then the battery is charged for 12 h to its maximum level. In all other cases, supplementary charging mode is used in which the single-board computer calculates the charging time according to the accumulated charge comsumption, which is determined by measuring the current when the battery was in use. Furthermore, the software also controls the amount of charge the battery receives in order to prevent overcharging and gas generation. If an alert occurs during charging, e.g., overheat (the battery temperature exceeds 70°C), the computer will stop the charging process

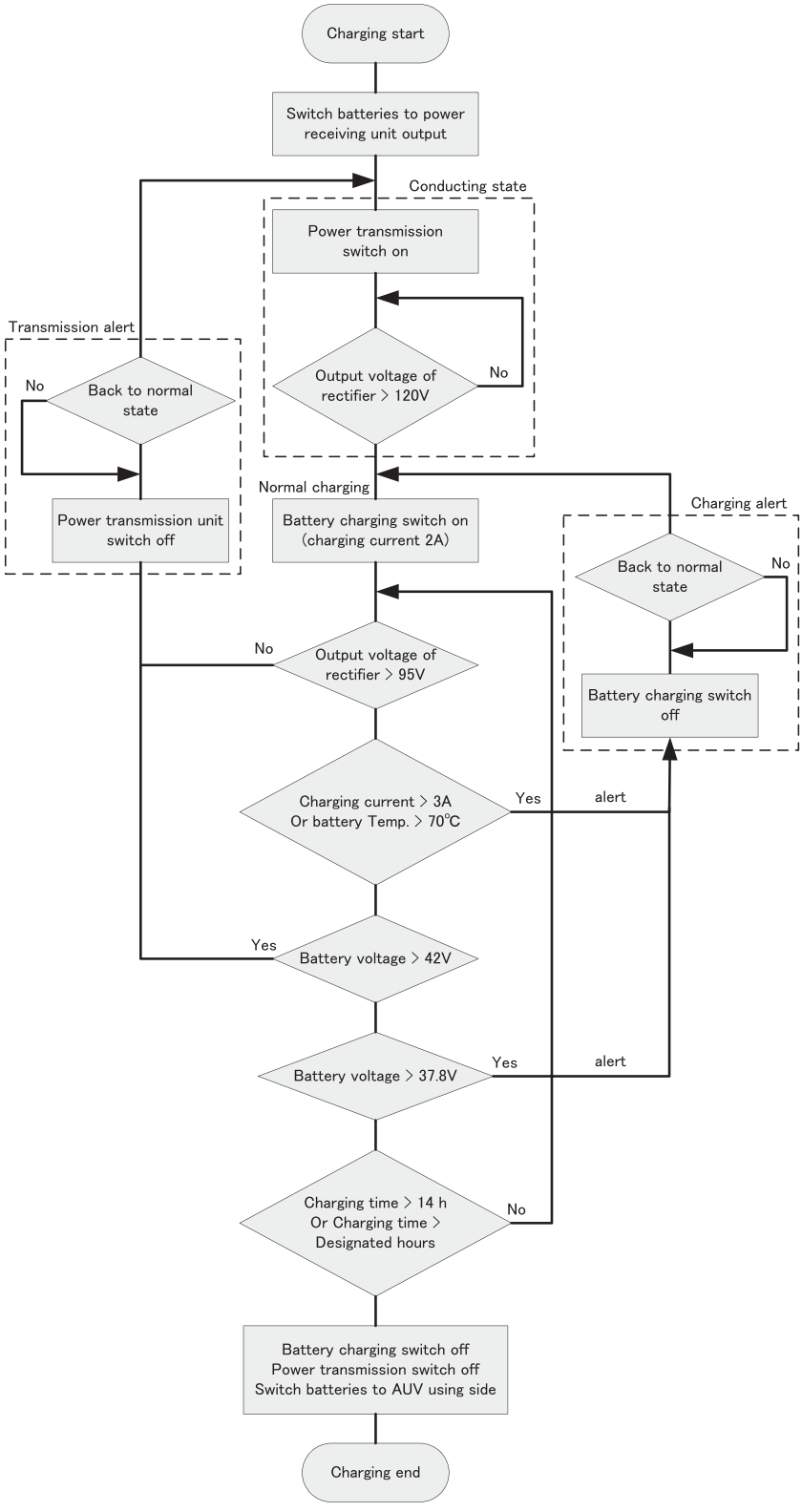

Fig. 5. Battery charging flowchart showing the sequence controlled by the single-board computer

and wait, automatically restarting the charging process after recovery of normal state.

A detailed flowchart of the charging control sequence is shown in Fig. 5. There are four states in the sequence, namely, the conducting state, normal charging state, transmission alert, and charging alert. The charging sequence starts from the conducting state in which the output voltage of the rectifier in the power receiving unit

is determined. If the output voltage of the rectifier exceeds 120 V, the battery charging switch will be turned on and the batteries will be charged with a constant charging current of 2 A. During this normal charging state, the battery voltages, battery temperatures, and charging current are monitored. If the charging current exceeds 3 A, the battery temperature becomes greater than 70°C, or the battery voltage exceeds 37.8 V, the system will enter the charging alert state in which battery charging will be switched off until the state goes back to normal. If the output voltage of the rectifier does not exceed 95 V or the battery voltage exceeds 42 V, it will enter the transmission alert state in which the power transmission switch is turned off until the state goes back to normal. After the charging time based on the previous current drain (or 14 h in full charge mode) has elapsed and the battery is fully charged, the battery charging switch and the power transmission switch will be turned off and the battery will be switched to AUV-use mode.

AUV battery charging experiment

An experiment was carried out in a water tank at the Underwater Technology Research Center, IIS, University of Tokyo, for 3 days from May 9 to 11 with a dummy underwater station in which a power transmission unit was set up as shown in Fig. 6. After removing the rear cover and the buoyancy material, we attached the power receiving unit. The experiment was started with fully charged batteries. With the power receiving unit attached, the AUV was moved around the tank to imitate observation mode. When the charge in the batteries became low, the single-board computer instructed the AUV to dock in the dummy station in order to charge the batteries. When the AUV approached the docking station, a wireless network was automatically established for communication. After the AUV docked, the single-board computer instructed the power transmission unit to switch on the power to charge the batteries using the wireless network. When the batteries were fully charged, a command was automatically sent to the power transmission unit to switch off the power.

In fact, we have developed a prototype high-bit-rate acoustic network with a 500-kHz carrier frequency for this geodetic observing robot system. At the time of the experiment, the acoustic network had not been miniaturized for installation into an AUV, so we used a radio network device instead. Although the radio network can only operate over a short distance in water, it functioned well in the proximate range. The development of an acoustic network will be reported in a future article.

Figure 7 shows the changes in the battery cell voltage over the charging time. The voltage increases from 1 V, and after an elapsed time of 11–12 h reaches its peak value. The cell voltage changes are very similar to the values provided in the battery manufacturer's data sheet. Figure 8 shows the changes in the cell temperature during the charging time. After the cell voltage reaches its peak value, the temperature increases. Based on Figs. 7 and 8, we can show that the maximum possible charging time for the Ni-Cd batteries in the AUV in full charge mode is 12 h, because the hydroxide-nickel electrode will emit oxygen gas if the charging time exceeds 12 h.

The voltage changes when the AUV was in observation mode are shown in Fig. 9. The voltage of the battery decreased as the observation time continued; when the

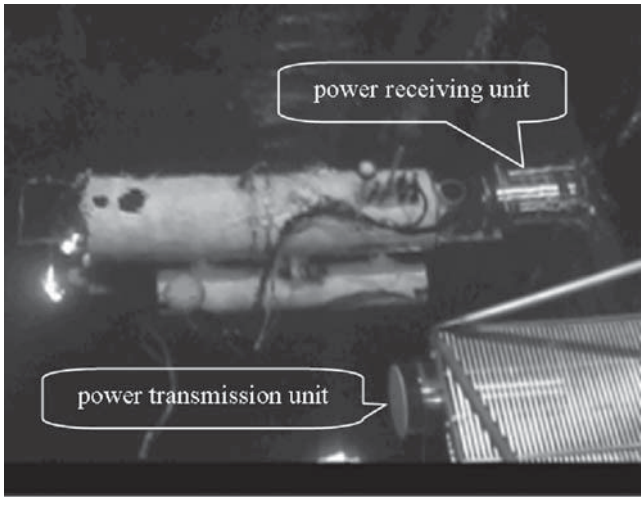

Fig. 6. AUV battery charging experiment

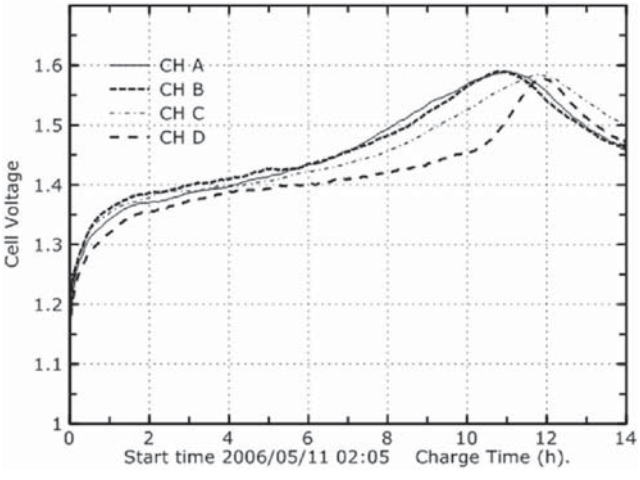

Fig. 7. Cell voltage change during the charging time; the voltage was monitored by a single-board computer. *CH A–D* represent the four sets of batteries in the experimental vehicle

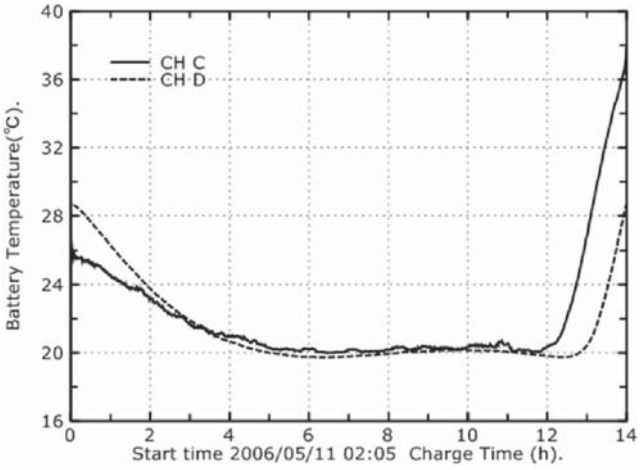

Fig. 8. Cell temperature change during the charging time; the temperature was monitored by a single-board computer

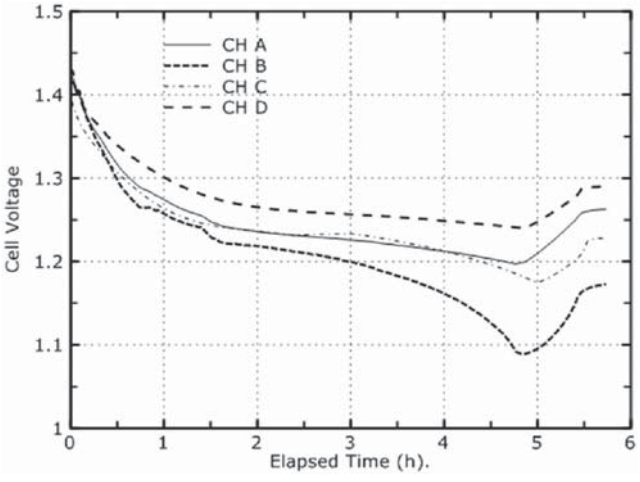

Fig. 9. Voltage change with the AUV in observation mode; the voltage was monitored by a single-board computer

threshold was exceeded, the AUV returned to the station to recharge its batteries. The results of this experiment provide evidence that the noncontact power supply system has excellent potential for AUV battery recharging.

Power transmission efficiency

Power transmission efficiency is a major consideration in the operation of a noncontact power supply system. In this study, we measured the transmission efficiency by connecting a constant-voltage electronic load to the power receiving unit output. The transmission efficiencies measured before the units were housed in watertight aluminum cylinders are shown in Table 2. Here, P_{in} is the input power of the transmission unit and P_{out} is the output power of the receiving unit. The power transmission efficiency (η) is calculated by the following formula:

$$\eta = P_{out} / P_{in} \quad (1)$$

It is clear from Table 2 that the power transmission efficiency reaches 80% when the coil gap between the transmission and receiving coils is 10 mm or less in air. After the units were housed in watertight aluminum cylinders, the power transmission efficiency was measured in different media such as air, freshwater, and salt water containing 33‰ salt. The results are shown in Table 3.

Compared with the value measured before the coils were placed in the cylinders, the transmission efficiencies decreased by 3%–4% in air for a 10-mm coil gap. This decrease is attributed to the occurrence of eddy currents because the distance between the coil and the aluminum cylinder is small.

From the data in this table, almost no difference was observed when the cylinders were placed in different media such as air, freshwater, and salt water. When the coil gap was 10 mm, the power transmission efficiency was 77%. By using improved materials that have a marginal influence on the electromagnetic induction, it is hoped that a power transmission efficiency of 80% can be achieved. Additionally, the noncontact high-power feeding system was designed and manufactured to meet the Japanese Electrical Appliances and Materials Safety Law.

Table 2. Transmission efficiency before the coils were housed in watertight cylinders

	Coil gap (mm)		
Item	8	10	13
P_{in} (W)	320	325	328
P_{out} (W)	260	260	260
Efficiency (η)	0.81	0.80	0.79

Table 3. Transmission efficiency after the coils were housed in watertight cylinders

	Coil gap (mm)			
Medium	10	12	14	16
Air	0.77	0.77	0.76	0.75
Freshwater	0.77	0.76	0.76	0.75
Salt water (33‰)	0.78	0.77	0.76	0.75

Conclusions

An efficient noncontact high-power feeding system of 400 W capacity and an inverting efficiency of 80% in air was developed for a seafloor geodetic observing robot network system. The potential and capabilities of the system were demonstrated by performing a water tank experiment in which the noncontact power supply and intelligently fed power to an AUV for 3 days. It is expected that the noncontact power supply system developed in this study will prove useful for various other underwater observation systems.

Acknowledgments. The authors would like to thank Yoshiaki Nose and Takashi Sakamaki for their help with the experiments at the Underwater Technology Research Center, IIS, University of Tokyo. This research was supported by the Ministry of Education, Culture, Sports, Science and Technology of Japan.

References

1. Asada A (2006) New approach to seafloor geodetic observation research: observation and future plans using AUVs (in Japanese). J Mar Acoust Soc Jpn 33(1):43–47
2. Asada A, Ura T, Han J, et al (2006) First sea trial of advanced seafloor geodetic observation system using autonomous underwater vehicles (in Japanese). In: Proceedings of the meeting of the marine acoustic society Japan, May 26, Tokyo, pp 89–92
3. Han J, Asada A, Ura T, et al (2006) High-speed acoustic network and noncontact power supplier for seafloor geodetic observing robot system (in Japanese). In: Proceedings of the meeting of the marine acoustic society Japan, pp 93–96
4. Han J, Asada A, Ura T, et al (2006) High-speed acoustic network and noncontact power supplier for seafloor geodetic observing robot system. IEEE, Oceans 2006, May 17, Singapore, p 94
5. Han J, Asada A, Ura T, et al (2006) Practical use examination of high-speed acoustic network and noncontact power supplier for a seafloor geodetic observing robot system (in Japanese). In: Proceedings of the meeting of the advanced marine science and technology society of Japan, May 19, Tokyo, pp 73–76
6. Kojiya T, Sato F, Matsuki H, et al (2004) Automatic power supply to underwater vehicles utilizing noncontact technology. In: Oceans '04 MTS/IEEE Techno-Ocean '04, Nov 9–12, Kobe, vol. 4, pp 2341–2345
7. Kawasaki T, Noguchi T, Fukasawa T, et al (2004) *Marine Bird*, a new experimental AUV: results of docking and electric power supply tests in sea trials. In: Oceans '04 MTS/IEEE Techno-Ocean '04, Nov 9–12, Kobe, vol. 3, pp 1738–1744
8. Fukasawa T, Noguchi T, Kawasaki T, et al (2003) *Marine Bird*, a new experimental AUV with an underwater docking and recharging system. In: Oceans 2003 Proceedings, Sept 25, San Diego, vol. 4, pp 2195–2200